

# The speed of mitochondrial movement is regulated by the cytoskeleton and myosin in *Picea wilsonii* pollen tubes

Maozhong Zheng · Qinli Wang · Yan Teng · Xiaohua Wang · Feng Wang · Tong Chen · Jozef Šamaj · Jinxing Lin · David C. Logan

Received: 8 September 2009 / Accepted: 4 December 2009 / Published online: 24 December 2009  
© Springer-Verlag 2009

**Abstract** Strategic control of mitochondrial movements and cellular distribution is essential for correct cell function and survival. However, despite being a vital process, mitochondrial movement in plant cells is a poorly documented phenomenon. To investigate the roles of actin filaments and microtubules on mitochondrial

movements, *Picea wilsonii* pollen tubes were treated with two microtubule-disrupting drugs, two actin-disrupting drugs and a myosin inhibitor. Following these treatments, mitochondrial movements were characterized by multiangle evanescent wave microscopy and laser-scanning confocal microscopy. The results showed that individual mitochondria underwent three classes of linear movement: high-speed movement (instantaneous velocities  $>5.0 \mu\text{m/s}$ ), low-speed movement (instantaneous velocities  $<5.0 \mu\text{m/s}$ ) and variable-speed movement (instantaneous velocities ranging from 0.16 to  $10.35 \mu\text{m/s}$ ). 10 nM latrunculin B induced fragmentation of actin filaments and completely inhibited mitochondrial vectorial movement. Jasplakinolide treatment induced a 28% reduction in chondriome motility, and dramatically inhibition of high-speed and variable-speed movements. Treatment with 2,3-butanedione 2-monoxime caused a 61% reduction of chondriome motility, and the complete inhibition of high-speed and low-speed movements. In contrast to actin-disrupting drugs, microtubule-disrupting drugs caused mild effects on mitochondrial movement. Taxol increased the speed of mitochondrial movement in cortical cytoplasm. Oryzalin induced curved mitochondrial trajectories with similar velocities as in the control pollen tubes. These results suggest that mitochondrial movement at low speeds in pollen tubes is driven by myosin, while high-speed and variable-speed movements are powered both by actin filament dynamics and myosin. In addition, microtubule dynamics has profound effects on mitochondrial velocity, trajectory and positioning via its role in directing the arrangement of actin filaments.

**Electronic supplementary material** The online version of this article (doi:10.1007/s00425-009-1086-0) contains supplementary material, which is available to authorized users.

M. Zheng · Q. Wang · X. Wang · F. Wang · T. Chen · J. Lin (✉)  
Key Laboratory of Photosynthesis and Molecular Environmental Physiology, Institute of Botany, Chinese Academy of Sciences, Xiangshan, 100093 Beijing, China  
e-mail: linjx@ibcas.ac.cn

M. Zheng · X. Wang · F. Wang  
Graduate School of Chinese Academy of Sciences, 100049 Beijing, China

Y. Teng  
Institute of Biophysics, Chinese Academy of Sciences, 100101 Beijing, China

J. Šamaj  
Department of Plant Cell Biology,  
Institute of Cellular and Molecular Botany,  
Rheinische Friedrich-Wilhelms-University Bonn,  
Kirschallee 1, 53115 Bonn, Germany

J. Šamaj  
Faculty of Science, Palacký University Olomouc,  
783 71 Olomouc, Czech Republic

D. C. Logan (✉)  
Department of Biology, University of Saskatchewan,  
Saskatoon, Saskatchewan S7N 5E2, Canada  
e-mail: david.logan@usask.ca

**Keywords** Actin filaments · Microtubules · Mitochondrial movement · Myosin · Trajectory · Velocity

## Abbreviations

EWM	Evanescence wave microscopy
LatB	Latrunculin B
Jas	Jasplakinolide
BDM	2,3-Butanedione 2-monoxime

## Introduction

Mitochondria are essential organelles responsible for energy supply (Bereiter-Hahn 1990), calcium homeostasis (Rizzuto et al. 2004; Yi et al. 2004) and intracellular signaling (Demaurex and Distelhorst 2003). Since the plant chondriome (all mitochondria in the cell) is organized as population of physically discrete organelles, the “discontinuous whole” (Logan 2006), mitochondrial function requires dynamic control of mitochondrial motility and distribution. It has been reported that mitochondrial motility varies considerably depending on the cell type and organism studied (Fehrenbacher et al. 2004; Miller and Sheetz 2006), presumably due to different mechanisms of mitochondrial movement. Such variability in motility likely has an impact on the role played by mitochondria in the different cell types. While many of the molecules involved in mitochondrial positioning and motility have been identified in animal systems (Trinczek et al. 1999; Minin et al. 2006), very little is known about these processes in plants (Van Gestel et al. 2002; Logan and Leaver 2000).

Distribution of mitochondria to strategic sites is dependent on a cytoskeleton-based transportation system. In plant cells, it has been demonstrated that mitochondria are associated with actin filaments (Olyslaegers and Verbelen 1998) and actin filaments are used as rails for mitochondrial transport (Van Gestel et al. 2002; Sheahan et al. 2005; Doniwa et al. 2007). However, studies on mitochondrial movement have focused on the dependence of mitochondrial movement on actin filaments (Van Gestel et al. 2002; Doniwa et al. 2007), or on actin filament function in mitochondrial fusion (Sheahan et al. 2005). Because no studies have focused systematically on the velocity of mitochondrial movement, the means by which mitochondrial velocity is regulated remains unknown.

Pollen tubes are exclusively tip-growing cells, in which vigorous cytoplasmic streaming maintains the delivery of various cell wall components to the tip where extension growth takes place (Cheung and Wu 2008). Tip-growing cells provide an ideal model for understanding organelle transport. Most previous studies on cytoplasmic streaming in pollen tubes have focused on the distribution of vesicles (Wang et al. 2005; Chen et al. 2007; Bove et al. 2008). To date, few studies on monitoring individual mitochondrial

transportation have been reported in living pollen tubes (de Win et al. 1999).

To provide further insight into the mechanisms underlying mitochondrial distribution, transport, and positioning we visualized mitochondrial movement immediately following treatment of *Picea wilsonii* pollen tubes with cytoskeleton-disrupting drugs. Specifically, we focused on inhibitor-induced alterations in the trajectory and velocity of mitochondrial movement.

## Materials and methods

### Plant material and in vitro pollen culture

Mature *Picea wilsonii* Mast pollen grains were collected from trees growing in the Botanical Garden of the Institute of Botany, Chinese Academy of Sciences in April 2004 and stored at  $-20^{\circ}\text{C}$  until use. For germination in vitro, pollen grains (1 mg/mL) were cultured in liquid medium (modified from Hao et al. 2005) containing 12.5% (w/v) sucrose, 0.01% (w/v)  $\text{H}_3\text{BO}_3$ , and 0.01% (w/v)  $\text{CaCl}_2$ . The pH of the medium was adjusted to 6.4 with phosphate buffered saline (PBS). Germination and elongation took place on a rotor (125 rpm) at  $25^{\circ}\text{C}$  in the dark.

### Staining of mitochondria

MitoTracker Red CMXRos was purchased from Molecular Probes (Molecular Probes, Eugene, OR, USA). Mitochondria were stained by the addition of MitoTracker Red to the culture medium at a final concentration of 500 nM. After 5 min incubation at  $25^{\circ}\text{C}$ , the culture medium was replaced with fresh medium lacking MitoTracker.

### Inhibitor treatments

All chemicals were purchased from Sigma (St Louis, MO, USA) unless stated otherwise. Stock concentrations of 1 mM latrunculin B (LatB), 1 mM taxol, and 100  $\mu\text{M}$  jasplakinolide (Jas) (Molecular Probes) were made in DMSO; 2,3-butanedione 2-monoxime (BDM) was prepared as a 500 mM stock solution in distilled  $\text{H}_2\text{O}$ ; oryzalin was prepared as a 20 mM stock in 100% ethanol. Appropriate volumes of stock solutions were added to pollen cultures after labeling with MitoTracker, to produce the following final concentrations: 10 nM LatB, 100 nM Jas, 100  $\mu\text{M}$  oryzalin, 5  $\mu\text{M}$  taxol, 50 mM BDM. Control treatments with solvents only [0.5% (w/v) DMSO or ethanol] had no visible effect on mitochondrial motility in *Picea wilsonii* pollen tubes (supplementary videos 1 and 2).

## Fluorescence labeling of cytoskeleton

Pollen tubes were cultured for 10 min in media containing 10 nM LatB, 100 nM Jas, 100  $\mu$ M oryzalin, 5  $\mu$ M taxol, or 50 mM BDM. Samples were then fixed at room temperature in 50 mM Pipes buffer (pH 6.9) containing 4% (w/v) paraformaldehyde for 1 h. For F-actin labeling, pollen tubes were incubated in 1% (v/v) Triton X-100 in PBS for 1 h and then incubated in 1  $\mu$ M phalloidin-TRITC in PBS (pH 6.9) buffer for 2–3 h in the dark. The immunolabeling of MTs was performed according to Sheng et al. (2006). Briefly, pollen tubes were permeabilized for 2–3 h in 1% Triton X-100/PBS after enzymatic digestion or freeze shattering. The resulting samples were then incubated with monoclonal antibody against  $\beta$ -tubulin (Sigma) and FITC-conjugated secondary antibody (Sigma). A control omitting primary antibody was also prepared. Thereafter, all the samples were washed, mounted on slides in 5% *n*-propyl gallate in glycerol, and observed under a Zeiss LSM 510 META laser-scanning confocal microscope (Zeiss, Jena, Germany), with an excitation wavelength of 488 nm and an emission wavelength of 522 nm.

## Microscopy

Evanescence wave microscopy (EWM) used the total internal reflection system which was constructed based on an inverted microscope (IX81 Olympus, Tokyo, Japan). Light from a multichannel argon laser (458, 488, 515 nm; 30 mW) was introduced to the microscope through a single mode fiber and three illumination lenses. The light was focused at the back focal plane of a high aperture objective lens (Apo 100 $\times$  OHR; NA 1.65; Olympus). A compact illumination device for total internal reflection fluorescence microscopy permitted variation of the angle of incident light from 0 $^\circ$  to 90 $^\circ$ . This allowed us to generate an axial resolution in the nanometer range. MitoTracker-labeled mitochondria in pollen tubes were visualized using an excitation wavelength of 514 nm with fluorescence emission being captured between 560 and 640 nm. Fluorescence was gathered through the objective at the optimal angle of the incident light. Time-lapse images were acquired every 50 or 200 ms through a frame grabber with genuine 16 Bit ( $2^{16}$ , 65536 gray levels).

Confocal images were obtained using a Zeiss LSM 510 META microscope, fitted with a 63 $\times$  water-immersion objective using an excitation wavelength of 514 nm and an emission wavelength of 560–640 nm.

## Data analysis

Analysis of images obtained by EWM was performed with Image-Pro Plus 5.1 (Media Cybernetics, Inc., San Diego,

CA, USA), Adobe Photoshop 7.0 (Adobe Systems), and ImageJ 1.34e (Wayne Rasband, National Institutes of Health, Bethesda, MD, USA). For analysis of lateral mobility, the imaging sequence was imported using Image J. For each image, the image was magnified and the outline of the mitochondrion to be tracked was traced enabling the centre of the organelle ( $x, y$ ) to be obtained. This operation was repeated three times and the mean co-ordinates ( $X, Y$ ) were taken to be the centre of the organelle at that moment in time. Displacement of mitochondria was calculated as a difference in the  $X$ - and  $y$ -coordinates over time. To enhance the visibility of the mitochondria, a high-pass Fast Fourier Transform filter followed by a  $3 \times 3$  pixel trimmed mean filter was applied to remove nonuniform background noise, and a flatten filter was used to smooth the background. The pixel size was 0.125  $\mu$ m with a 1.6 $\times$  optical zoom, and the image size was typically 326  $\times$  484 pixels. The fluorescence intensity was expressed in the 8-bit value of digitization as previously described (Tsuboi et al. 2000; Taraska and Almers 2004).

## Results

### Effect of actin- and microtubule-disrupting drugs on chondriome mobility

To decipher the regulation of mitochondrial movement by microtubules, actin filaments and myosin, two microtubule-disrupting drugs, oryzalin and taxol, and two actin-disrupting drugs, LatB and Jas together with the myosin inhibitor, BDM, were used to treat pollen tubes. At first, the effects of these inhibitors on the motility of the chondriome were investigated. According to the approach established by Yi et al. (2004), two time-lapse confocal microscopy images were captured 10 s apart, the first image was false-colored green while the second was colored red and then the two were merged (Fig. 1). In the merged image, the yellow (green + red) pixels represent mitochondria that maintained their position, whereas the green and red pixels indicated the sites of movement, including movement into or out of the focus plane. The number of green and red pixels, expressed as a percentage of the total number of pixels counted is used to represent mitochondrial motility.

In control pollen tubes, statistical analysis showed that 80.1% ( $n = 18$  pollen tubes, 3,648 mitochondria) of mitochondria moved within 10 s in normal pollen tubes (Figs. 1a, 2). When G-actins were sequestered by 10 nM LatB, chondriome motility was reduced by 82.2% ( $n = 18$  pollen tubes, 3,499 mitochondria,  $P < 0.01$ ) (Fig. 2). Only a few mitochondria kept moving in the subapical area but movement of mitochondrial into the apical region was inhibited (Fig. 1b, compared with a). When 100 nM Jas

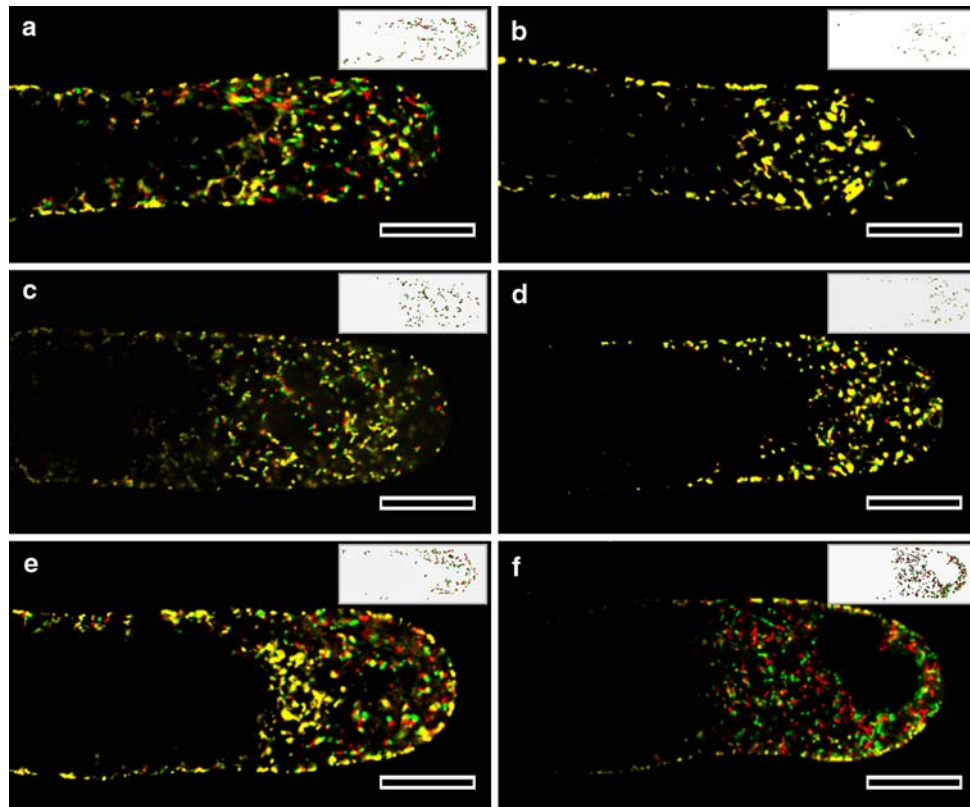


**Fig. 1** Effects of LatB, Jas, BDM, taxol and oryzalin on mitochondrial motility in *Picea wilsonii* pollen tube. *Green/red* overlay of two time-lapse confocal images ( $\Delta t = 10$  s) of Mitotracker fluorescence in a pollen tube before and 10 min after addition of inhibitors. **a** Control pollen tubes cultured for 18 h. **b** Pollen tubes treated with 10 nM LatB. Note the near complete inhibition of mitochondrial movement (demonstrated by near-complete overlay of the two color signals) and presence of few mitochondria in the apical region. **c** Pollen tubes treated with

100 nM Jas. **d** Treated with 50 mM BDM, showing an inhibition of mitochondrial motility. **e** Pollen tubes treated with 5  $\mu$ M taxol. Note that most mitochondrial movement occurred in the cortical cytoplasm. **f** Pollen tubes treated with 100  $\mu$ M oryzalin. Note the vacuole appearance in the apical region and increase in mitochondrial motility. *Inserts* represent corresponding processed images showing only the pixels whose values differ by more than a threshold value (+ and -) between the two time points (*bars* 20  $\mu$ m)

was used to inhibit F-actin turnover, a 27.6% ( $n = 19$  pollen tubes, 3,771 mitochondria,  $P < 0.01$ ) decrease was found in mitochondrial motility (Fig. 2). This kind of decrease was primarily limited to the shank of the pollen tubes (Fig. 1c).

Pollen tubes were treated with the myosin inhibitor, BDM, to test the dependence of mitochondrial motion on myosin. The result showed that treatment with 50 mM BDM for 10 min caused a 61% ( $n = 18$  pollen tubes, 3,531 mitochondria,  $P < 0.01$ ) reduction in mitochondrial motility (Figs. 1d, 2). Given that either Jas, or BDM alone did not completely inhibit mitochondrial motility, pollen tubes were treated with a combination of BDM and Jas to determine whether, or not, the residual mitochondrial movement in the pollen tubes treated with BDM could be completely inhibited by Jas. The result showed that mitochondrial motility was reduced by 89% ( $n = 16$  pollen tubes, 3,437 mitochondria,  $P < 0.01$ ) in pollen tubes treated with both Jas and BDM, a percentage similar to the sum of those measured following individual treatment with Jas or BDM (Fig. 2).

In contrast to actin-disrupting drugs, which caused significant alterations in chondriome motility, disruption of microtubules by treatment with the inhibitors oryzalin or taxol led to more moderate alterations in mitochondria motility. Taxol treatment at concentrations of 5  $\mu$ M for 10 min reduced mitochondrial motility to 86% ( $n = 17$  pollen tubes, 3,372 mitochondria,  $P < 0.05$ ) of that measured in control pollen tubes (Fig. 2). Interestingly, while mitochondrial motility was inhibited in the inner cytoplasm of the subapical region, mitochondrial motility in the cortical cytoplasm was slightly enhanced (Fig. 1e; supplementary video 3 compared with supplementary video 4). Intriguingly, the microtubule-depolymerizing drug, oryzalin, affected mitochondrial motility in an opposite manner relative to the microtubule-stabilizing drug, taxol. Treatment with 100  $\mu$ M oryzalin for 10 min disrupted cytoplasmic organization (Fig. 1f), and caused an increase in mitochondrial motility of 9.5% ( $n = 18$  pollen tubes, 3,578 mitochondria,  $P < 0.05$ ; Fig. 2).



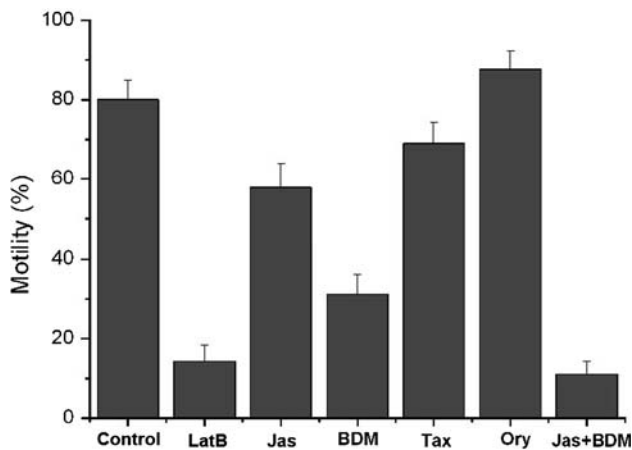


**Fig. 2** Mitochondrial motility in the presence of various inhibitors. The data were calculated from a *green/red* overlay of two time-lapse confocal images ( $\Delta t = 10$  s). Motility is calculated from the number of *red* and *green* pixels expressed as a percentage of the total number of colored pixels. All data represent mean  $\pm$  SD from 16 to 19 pollen tubes

Detection of three classes of mitochondrial linear movement in control pollen tubes

In order to distinguish the effects of various inhibitors, mitochondrial movements were further observed using EWM. EWM has provided valuable information about organelle trafficking, especially in living cells, under lengthy observation periods (Wang et al. 2006). Using EWM, the movement of individual mitochondria was recorded at 200 ms intervals, which is 15-fold faster than that in any previous study. Supplementary video 5 shows that mitochondrial movement in untreated control pollen tubes varied from small continuous oscillations to large-scale displacements of tens of micrometers within seconds. Mitochondrial *x*–*y* plane velocities and trajectories were analyzed using Image J software. The results showed that mitochondria in untreated pollen tubes moved at variable instantaneous velocities. Among these instantaneous velocities, 5  $\mu\text{m/s}$  appeared as a threshold, within the recording timescale, relative to which three types of mitochondrial linear movements could be classified: consistently low-speed movement ( $<5 \mu\text{m/s}$ ), consistently high-speed movement ( $>5 \mu\text{m/s}$ ), and variable-speed movement when the mitochondrion’s instantaneous velocity fluctuated from low to high values within the recording period. In untreated pollen tubes, 66% of mitochondria were observed undergoing low-speed movement (Table 1), with an average velocity of  $1.42 \pm 0.85 \mu\text{m/s}$  (Fig. 3a). The displacement of mitochondria undergoing low-speed movement could reach 31.45  $\mu\text{m}$  within a 20-s period (Fig. 3b). Mitochondria were measured moving with high-speed movement in 6.4% of cases (Table 1), with an average velocity of  $7.1 \pm 1.5 \mu\text{m/s}$

**Table 1** Frequency of the three classes of mitochondrial movement

	Low-speed movement (%)	High-speed movement (%)	Variable-speed movement (%)
Untreated control	66.0	6.4	27.6
10 nM LatB	98.3	0	1.7
100 nM Jas	91.2	1.3	7.5
50 mM BDM	9.5	1.1	89.4
5 $\mu\text{M}$ Tax	35.7	7.1	57.2
100 $\mu\text{M}$ Ory	58.8	5.1	36.1

The frequencies were calculated following observation by EWM of 200 individual organelles within five living pollen tubes per treatment. Classification of movement was based on the instantaneous velocity of mitochondria during the period of observation (which varied depending on the speed of movement due to movement out of the focal plane). Low-speed movement: consistently  $<5 \mu\text{m/s}$ ; high-speed movement: consistently  $>5 \mu\text{m/s}$ ; variable-speed movement: instantaneous velocity fluctuating from low to high values within the period of observation

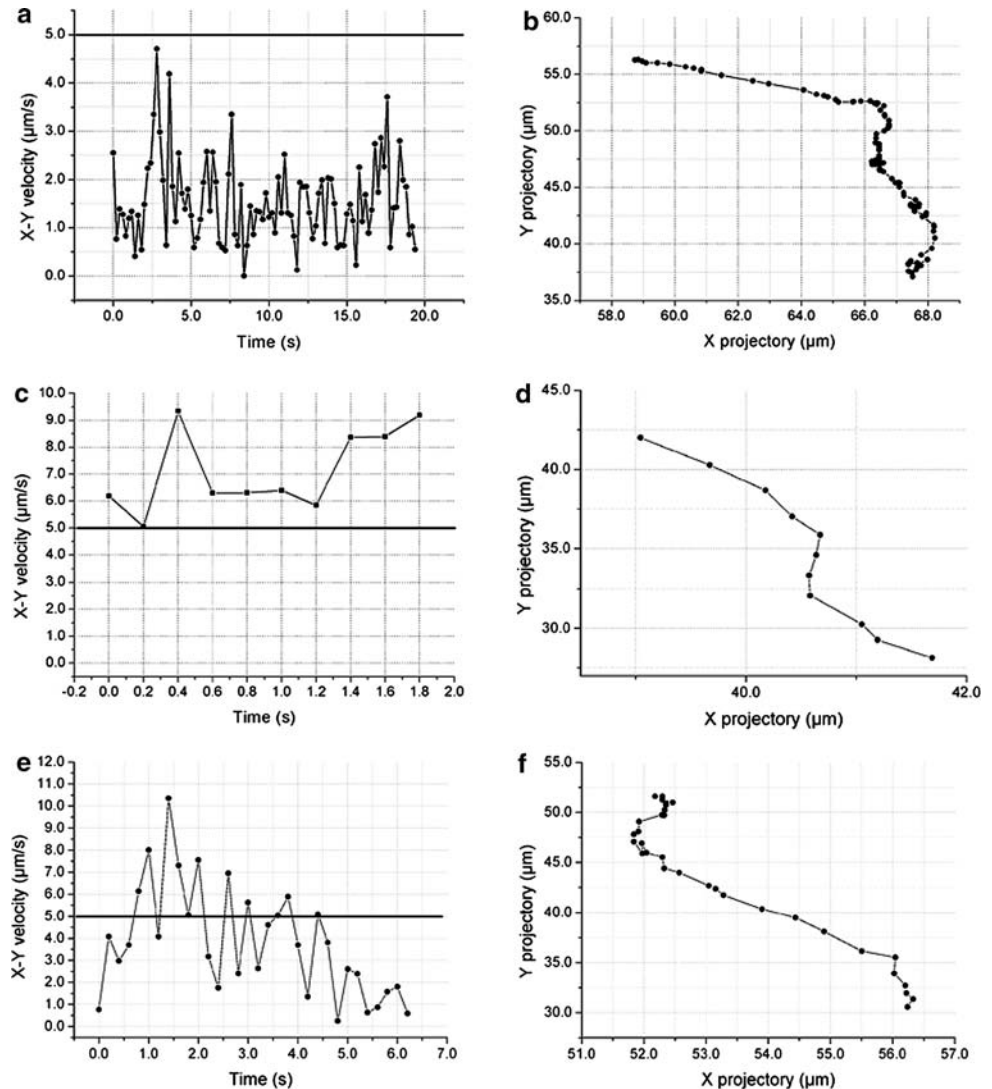
(Fig. 3c). High-speed movement would typically last only several seconds, but within that time would result in displacements of tens of micrometers (Fig. 3d). Finally, 27.6% of mitochondria moved with variable speed (Table 1). Mitochondria undergoing variable-speed movement (Fig. 3e) could be displaced by 24.56  $\mu\text{m}$  within a 6.2 s period (Fig. 3f). In fact, when observed over a 5-min period (only possible when the mitochondrion remained in the focal plane) mitochondria were frequently seen to move sequentially with the characteristics of each of three movement classes for various lengths of time.

Changes to the three classes of mitochondrial movement by drug treatments

As described above, various drug treatments were found to result in reductions in mitochondrial motility. Mitochondria in drug-treated pollen tubes were observed by EWM in order to analyze the nature of the residual mitochondrial movements. Approximately 200 mitochondria in five pollen tubes per treatment were analyzed. In LatB-treated pollen tubes, linear mitochondrial movement was almost completely arrested (Table 1; Fig. 2). The residual mitochondrial motion is best termed “wiggling”: mitochondrial displacement was restricted to an area of 1.4–3.6  $\mu\text{m}^2$  (Fig. 4a) and the mitochondria wiggled at an average velocity of  $0.70 \pm 0.36 \mu\text{m/s}$  (Fig. 4b). In pollen tubes treated with Jas, mitochondrial movement at instantaneous velocities within the high-speed and variable-speed classes was greatly inhibited (Table 1); residual mitochondrial movements were within the low-speed class ( $>5 \mu\text{m/s}$ ) with an average velocity of  $1.28 \pm 0.77 \mu\text{m/s}$  (Fig. 4c, d).

In contrast to treatment with Jas, which inhibited most of the variable-speed and high-speed movements,

**Fig. 3** Three classes of mitochondrial movements in pollen tubes cultured in normal medium. Mitochondrial linear movements in a single focal plane were recorded as described in “Materials and methods”. The data are calculated from observations of one typical individual mitochondrion. **a** Plot of the  $x$ - $y$  velocity of a mitochondrion exhibiting low-speed movement. **b** The lateral mobility of the same mitochondrion as in **a** as a plot of  $x$  versus  $y$  coordinates. **c** Plot of the  $x$ - $y$  velocity of a mitochondrion exhibiting high-speed movement. **d** The lateral mobility of the same mitochondrion as in **c** on a plot of  $x$  versus  $y$  coordinates. **e** Plot of the  $x$ - $y$  velocity of a mitochondrion exhibiting variable-speed movement. **f** The lateral mobility of the same mitochondrion in **e** on a plot of  $x$  versus  $y$  coordinates



BDM treatment eliminated movement within the high-speed (consistently  $>5 \mu\text{m/s}$ ) and low-speed (consistently  $<5 \mu\text{m/s}$ ) classes (Table 1). The residual vectorial mitochondrial movement following treatment with BDM fell within the variable-speed class (moving with instantaneous velocities both greater- and less-than  $5 \mu\text{m/s}$  within the recording timeframe) with a maximal velocity of  $7.02 \mu\text{m/s}$  (Fig. 5a): approximately 83% of the maximum velocity measured in control pollen tubes. The plot of the  $x$ - $y$  coordinates of mitochondria showed that individual organelles frequently changed direction during movement (Fig. 5b).

In pollen tubes treated with taxol, the percentage of mitochondria moving at instantaneous velocities within the low-speed class was reduced (Table 1) while the majority of residual mitochondrial movements were classifiable as variable-speed with an average velocity of  $3.68 \pm 2.85 \mu\text{m/s}$  (Fig. 6a), representing an approximate 50% increase over

control. This increase in the instantaneous velocity of mitochondria moving within the variable-speed class was consistent with our observations that mitochondrial motility in the cortical cytoplasm was slightly enhanced. Furthermore, the average displacement of mitochondria moving within the low-speed class was reduced to  $5.31 \pm 1.51 \mu\text{m}$  by taxol (Fig. 6b). Interestingly, oryzalin treatment had little effect on velocity (Table 1; Fig. 7a, c, e), but instead had a dramatic affect on mitochondrial trajectories (Fig. 7b, d, f; supplementary video 6).

#### Velocity distribution of the residual mitochondrial movements

In order to confirm the observed changes to the three classes of mitochondrial movements measured by quantifying the instantaneous velocity and displacement of individual mitochondria, we plotted the frequency distribution of the

**Fig. 4** Effects of F-actin inhibitors on the movement of an individual mitochondrion. Mitochondrial linear movements in a single focal plane were recorded as described in “Materials and methods”. The data are calculated from observations of one typical individual mitochondrion. **a** The lateral mobility of a wiggling mitochondrion in a LatB-treated (10 nM for 10 min) pollen tube as a plot of  $x$  versus  $y$  coordinates. **b** Plot of the  $x$ – $y$  velocity of a wiggling mitochondrion in a LatB-treated pollen tube. **c** The lateral mobility of a mitochondrion in a Jas-treated (100 nM for 10 min) pollen tube as a plot of  $x$  versus  $y$  coordinates. **d** Plot of the  $x$ – $y$  velocity of a mitochondrion in a Jas-treated pollen tube

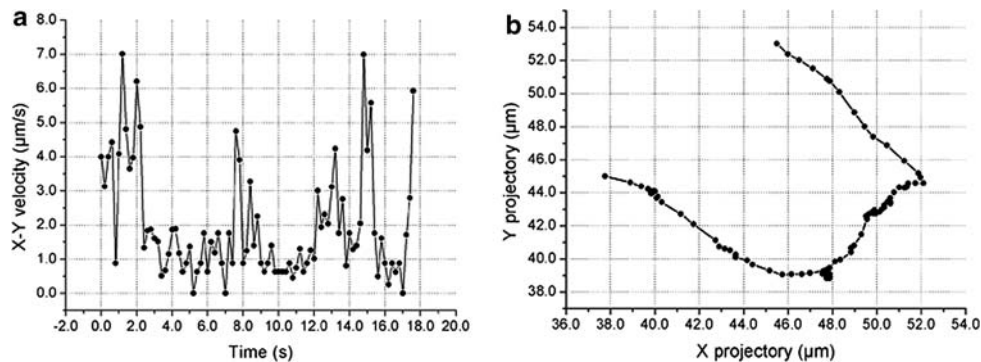
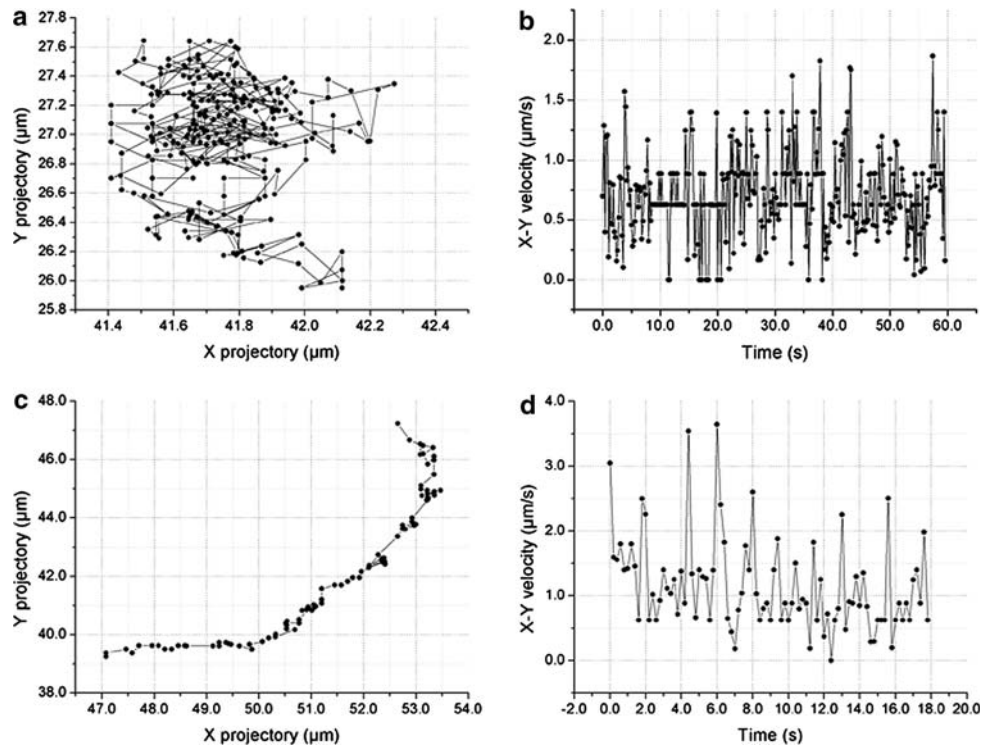


**Fig. 5** Effects of the myosin ATPase inhibitor BDM on the movement of an individual mitochondrion. Mitochondrial linear movements in a single focal plane were recorded as described in “Materials and methods”. The data are calculated from observations of one typical individ-

ual mitochondrion. **a** The lateral mobility of a mitochondrion in a BDM-treated (50 mM for 10 min) pollen tube as a plot of  $x$  versus  $y$  coordinates. **b** Plot of the  $x$ – $y$  velocity of a mitochondrion in a BDM-treated pollen tube

average velocities of mitochondria ( $n > 100$ ) in untreated and drug-treated pollen tubes. After treatment with LatB, mitochondria were unable to move at velocities  $>3.0 \mu\text{m/s}$ , 88% of mitochondrial movements were at average velocities of  $0.5$ – $1.999 \mu\text{m/s}$  (Fig. 8a compared with b). Following treatment with Jas, residual mitochondrial movements were skewed toward lower velocities: 59% of mitochondria moved at average velocities of  $1.0$ – $1.999 \mu\text{m/s}$  and 14% of mitochondria moved at average velocities of  $>3.0 \mu\text{m/s}$  (Fig. 8c). In pollen tubes treated with BDM, residual mitochondrial movements were skewed toward high velocities, there was no movement at average velocities of  $0.5$ – $0.999 \mu\text{m/s}$  and 49% of mito-

chondria moved at average velocities of  $>3.0 \mu\text{m/s}$  (Fig. 8d). When treated with taxol, the percentage of mitochondria moving at average velocities of  $>2.0 \mu\text{m/s}$  increased (Fig. 8e). After treatment with oryzalin, the distribution of velocities was similar to that seen in control pollen tubes, except that the percentage of mitochondria moving at average velocities of  $1.0$ – $1.999 \mu\text{m/s}$  increased slightly and the percentage moving at velocities of  $0.5$ – $0.999 \mu\text{m/s}$  was slightly reduced (Fig. 8f). All these results demonstrate that the frequency distributions of mitochondrial average velocities were in agreement with the measured changes in the instantaneous velocity class when individual mitochondria were tracked.



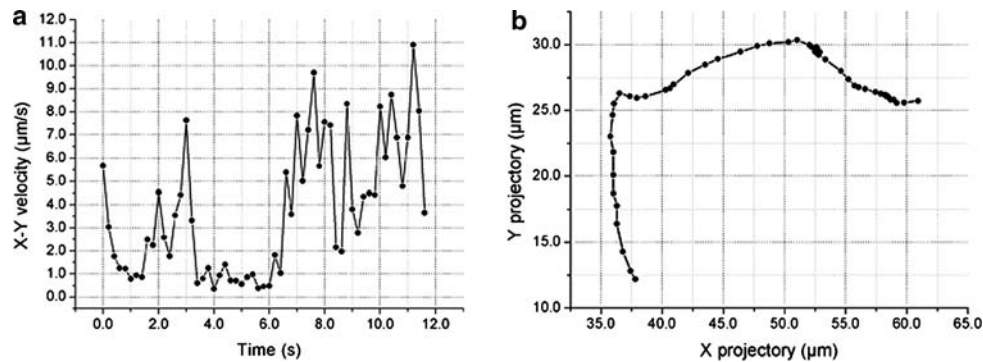
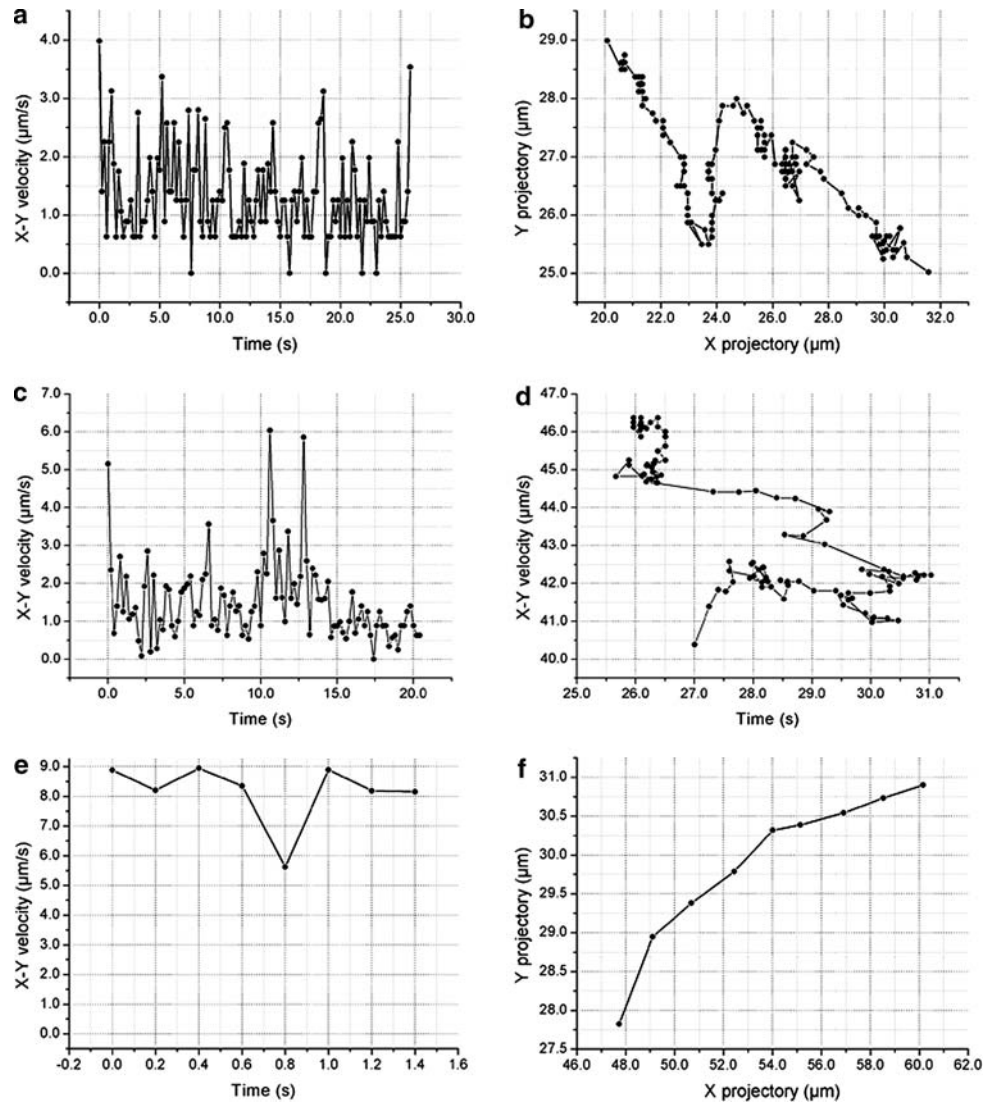


**Fig. 6** Effects of taxol on the movement of an individual mitochondrion. Mitochondrial linear movements in a single focal plane were recorded as described in “Materials and methods”. The data are calcu-

lated from observations of one typical individual mitochondrion. **a** The lateral mobility of a mitochondrion as a plot of  $x$  versus  $y$  coordinates. **b** Plot of the  $x$ - $y$  velocity of the same mitochondrial movement as in **a**

**Fig. 7** Effects of oryzalin on the movement of an individual mitochondrion. Mitochondrial linear movements in a single focal plane were recorded as described in “Materials and methods”. The data are calculated from observations of one typical individual mitochondrion. The data show the mitochondrion exhibiting low-speed movement (**a**), variable-speed movement (**c**), and high-speed movement (**e**). The data are also presented as a plot of  $x$  versus  $y$  coordinates: low-speed movement (**b**), variable-speed movement (**d**), and high-speed movement (**f**)



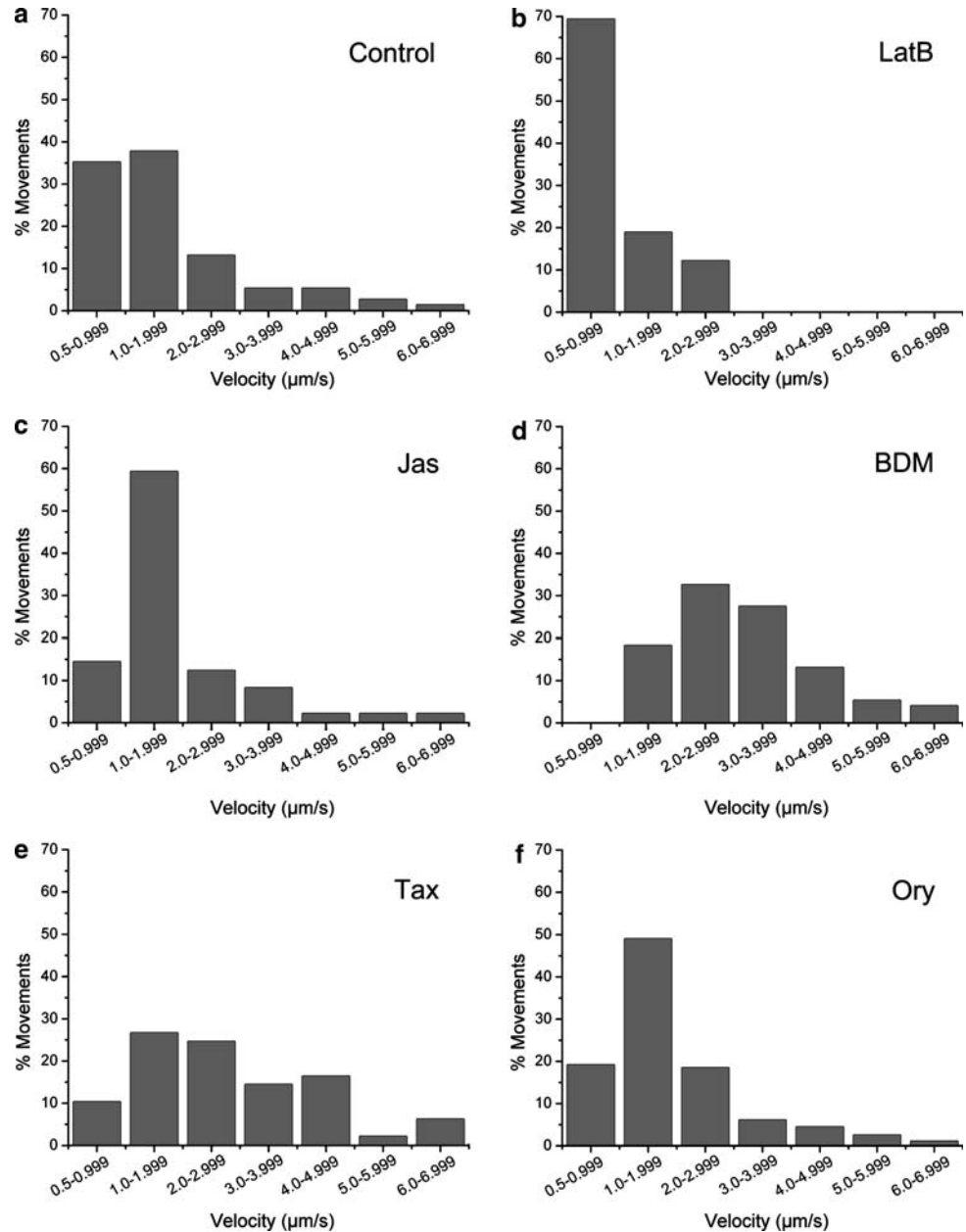
#### Effects of inhibitors on the pollen tube cytoskeleton

To evaluate the effects of the inhibitors LatB, Jas, BDM, taxol and oryzalin on the actin cytoskeleton, we performed

confocal microscopy of pollen tubes stained with phalloidin-TRITC. AFs of untreated pollen tubes incubated in culture medium for 18 h showed straight or slightly helical actin bundles oriented in an axial array. Abundant arrays of fine



**Fig. 8** Frequency distribution of average velocities of mitochondrial movements in control and inhibitor-treated pollen tubes. Mitochondrial linear movements in a single focal plane were recorded as described in “Materials and methods” and graphed as a function of frequency within distinct velocity categories ( $n > 100$ ). **a** Mitochondrial moved at various velocities in untreated pollen tubes. **b** Mitochondrial movements with high velocity disappeared in pollen tubes treated with 10 nM LatB for 10 min. **c** The distribution of velocities of the residual mitochondrial movements was skewed toward the slower velocities in pollen tubes treated with 100 nM Jas for 10 min. **d** The distribution of velocities of the residual mitochondrial movements was skewed toward the higher velocities in pollen tubes treated with 50 mM BDM for 10 min. **e** Treatment with 5  $\mu$ M taxol for 10 min resulted in the residual mitochondrial movements being faster than that measured in control pollen tubes. **f** Treatment with 100  $\mu$ M oryzalin for 10 min caused little affect on the distribution of velocities



filaments were frequently observed about 20  $\mu$ m behind the tube apex, and a few thick filaments extended into the apex (Fig. 9a). In the presence of 10 nM LatB for 10 min, the apical and subapical fine AFs were completely eliminated, resulting in diffuse fluorescent aggregates of phalloidin-stained material: only a few very short AFs are visible in the basal region (Fig. 9b). Application of 100 nM Jas for 10 min resulted in a slight increase in the numbers of thick actin bundles in the shank of pollen tube and a decrease in the numbers of fine AFs in the apical zone (Fig. 9c). When treated with 50 mM BDM for 10 min, there was no obvious alteration in the actin cytoskeleton (Fig. 9d). The staining also revealed that the microtubule inhibitors affected the organization of AFs in pollen tubes. AFs appeared more

bundled but less numerous following treatment with 5  $\mu$ M taxol for 10 min compared with those in control pollen tubes, and these actin bundles extended throughout the pollen tube apex replacing the fine AFs (Fig. 9e). In contrast to treatment with taxol, a 10 min treatment with 100  $\mu$ M oryzalin reduced the appearance of fine AFs in the apex but stimulated the appearance of curved and helical actin bundles in the shank, especially in the subapical region (Fig. 9f).

**Discussion**

Mitochondrial transport is likely controlled to fit a local demand for the supply of energy and to enable mitochondrial

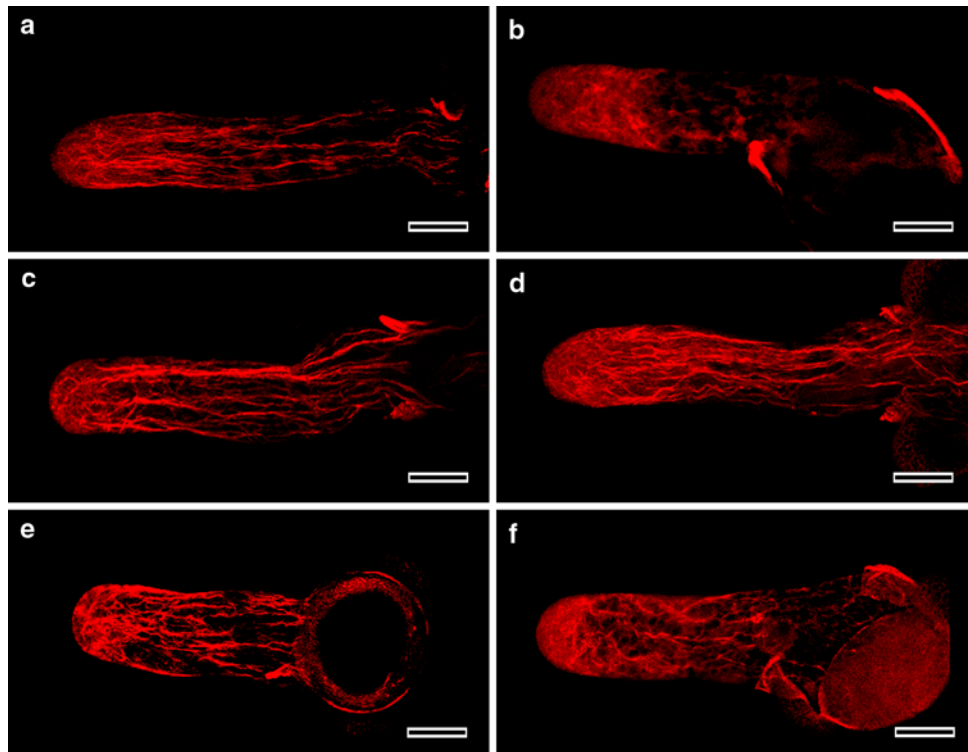


**Fig. 9** Effect of LatB, Jas, BDM, taxol and oryzalin on F-actin in *Picea wilsonii* pollen tubes. Samples were chemically fixed and stained with TRITC-phalloidin. All pollen tubes were visualized by confocal microscopy; the images are projections of 30–50 optical sections at 0.5- or 1- $\mu\text{m}$  intervals in the Z-axis. **a** Untreated pollen cultured in standard medium for 18 h showing a long pollen tube and normal organization of actin filaments and bundles. **b** Pollen tube treated with 10 nM LatB for 10 min, showing the elimination of visible apical and subapical fine actin filaments and diffuse aggregates of phalloidin-stained

material. **c** Pollen tube treated with 100 nM Jas for 10 min. Note a slight increase of thick actin bundles in the shank and a decrease of fine actin filaments in the apical zone. **d** Pollen tube treated with 50 mM BDM for 10 min, no obvious alteration in the actin cytoskeleton was observed. **e** Pollen tube treated with 5  $\mu\text{M}$  taxol for 10 min. Note more bundled but less abundant actin filaments. **f** Pollen tube treated with 100  $\mu\text{M}$  oryzalin for 10 min, showing curved and helical actin bundles (bars 20  $\mu\text{m}$ )

participation in cell signaling. However, little is known concerning the mechanics of plant mitochondrial transport. In the axons and dendrites of cultured hippocampal neurons, Ligon and Steward (2000) found that mitochondrial velocities varied in different regions. Furthermore, Miller and Sheetz (2006) found that high-velocity mitochondrial transport decreased and low-velocity transport increased in a proximodistal gradient along the axon of cultured chicken dorsal root ganglion neurons. In yeast, it has been reported that mitochondria move at various velocities (Fehrenbacher et al. 2004). In present study, we found three classes of linear mitochondrial movements in *Picea wilsonii* pollen tubes during the recording period: (a) high-speed movement, in which mitochondria move at consistently high instantaneous velocities ( $>5.0 \mu\text{m/s}$ ), (b) low-speed movement, in which mitochondria move at consistently low instantaneous velocities ( $<5.0 \mu\text{m/s}$ ) (c) variable-speed movement, in which mitochondria move with variable velocity ( $>5 \mu\text{m/s}$  and  $<5 \mu\text{m/s}$  within the recording period). These results suggest that mitochondria of plant, animals and yeast

share a common requirement for the ability to move through the cell at variable velocities.

At least three types of actin-based intracellular organelle motility have been described: (a) motility driven by motor proteins, whereby mitochondrial movement is powered by myosins moving along actin filaments (Tominaga et al. 2003), (b) motility using a comet tail structure, whereby mitochondrial movement is driven by actin filament elongation via actin filament plus-end polymerization (Drams and Cossart 1998) and (c) motility using actin filament flow, whereby actin filaments serve as “conveyor belts” to drive mitochondrial movement (Fehrenbacher et al. 2004). In the present study, 34% of mitochondria analyzed moved with instantaneous velocities higher than  $5 \mu\text{m/s}$ , and some with maximum velocities of  $11 \mu\text{m/s}$ , which is higher than the previously reported fastest processive movement driven along actin filaments by myosin XI ( $7 \mu\text{m/s}$ ) (Tominaga et al. 2003). Furthermore, our results showed that vectorial movements of mitochondria cannot be inhibited completely by treatment with 50 mM BDM or 100 nM Jas, but can be inhibited completely by a combined treatment of BDM and

Jas. This result is in agreement with the results of our previous study of mitochondrial movement in *Arabidopsis* root hairs (Zheng et al. 2009). Moreover, EWM demonstrates that BDM and Jas inhibited specific classes of mitochondrial movement rather than having a blanket inhibitory effect which would be expected if all mitochondrial movement was driven by myosin alone. Together our data suggest that mitochondrial movements are driven by both myosin and actin filaments flow in *Picea wilsonii* pollen tubes.

Myosins are motor proteins that slide along actin filaments using energy provided by the hydrolysis of ATP. Reddy and Day (2001) have reported that there are 17 *Arabidopsis* myosins: 4 within the myosin VIII class, and 13 within the myosin XI class. Among the 13 myosin XI members, only one has been shown by homologous transient gene knock-out experiments to have a major role in the movement of mitochondria (Avisar et al. 2008). In addition, it has been shown that mitochondrial movements remained, although they were reduced, in a myosin knock-out mutant (Peremyslov et al. 2008; Prokhnovsky et al. 2008). Furthermore, heterologous expression of dominant negative forms of *Arabidopsis* myosins lacking the actin binding domain failed to completely inhibit mitochondrial movement (Sparkes et al. 2008). While these reports suggest functional redundancy among the *Arabidopsis* myosin family they also suggest that other mechanisms, e.g., actin turnover or treadmilling, may be important in driving mitochondrial movement. In present study, it was interesting that treatment with 50 mM BDM had a greater inhibitory effect on low-speed and high-speed movements than on mitochondria moving with variable velocities within the recording timeframe. Although BDM inhibits ATPases in addition to myosins, the parsimonious explanation for BDM inhibition of mitochondrial movement is through inhibition of myosin activity and therefore that low-speed and high-speed movements in *Picea* pollen tubes are primarily myosin-driven.

Actin filaments comprise a dynamic system in plant cells. Staiger et al. (2009) showed that actin filaments in *Arabidopsis* epidermal cells exhibited a high growth rate (1.7  $\mu\text{m/s}$ ) and possess severing activity. In addition, Staiger et al. (2009) found that actin filaments underwent buckling and straightening events, indicative of filament–filament sliding and/or resulting from tension along a filament. These observations hinted that actin filament dynamics have the power to drive mitochondrial movement at rates of several microns per second. Recently, it was shown that actin filament dynamics are essential for myosin-based transport of organelles in *Xenopus* melanophores (Semenova et al. 2008). In the present study, when actin filament turnover was inhibited by Jas, variable-speed and high-speed movements of mitochondria were abolished,

suggesting that actin filament dynamics was involved in driving movement in these two categories.

In *Picea wilsonii* pollen tubes, using the methods of Sheng et al. (2006), microtubules were found to form a network around the cortical cytoplasm (supplemental Fig. S1). Although microtubules were much less evident in pollen tubes treated with oryzalin (supplemental Fig. S1) linear mitochondrial movement was unaffected suggesting that the complex microtubule network in *Picea wilsonii* pollen tubes does not serve as a track for mitochondrial movements. However, we found that taxol treatment induced the appearance of more AF bundles extending into the pollen tube apex and reduced the number of fine AFs. Simultaneously, enhanced mitochondrial motility could be observed in the cortical cytoplasm. In contrast, oryzalin treatment induced the appearance of curved and helical actin bundles, subsequently leading to curved mitochondrial trajectories. These phenomena cannot be explained simply by the secondary effect of a change in cytosol viscosity since there was little measured change in mitochondrial velocity upon treatment with microtubule-active drugs, and oryzalin treatment resulted in the movement of vacuoles into the apical region of pollen tubes suggesting a decrease rather than an increase in cytosol viscosity. Microtubules have been shown to determine the proper placement of actin polymerization in root hair cells (Tominaga et al. 1997; Sieberer et al. 2005). Formins are actin-nucleating proteins that stimulate the de novo polymerization of actin filaments (Cheung and Wu 2004). In yeast, it was reported that microtubule plus-ends transport the formin regulators tea1p and tea4p via association with tea2p (kinesin) and tip1p (CLIP-170) (Basu and Chang 2007). Homologs of these yeast proteins are present in the *Arabidopsis* genome (Sieberer et al. 2005), suggesting conservation of the role of microtubules in directing the proper placement of actin polymerization through the transport of formin regulators. Given the link between microtubule plus-ends and formin (Sieberer et al. 2005; Basu and Chang 2007), and the link between actin filament organization and formin, we speculate that alterations in microtubule dynamics lead directly to a redistribution of formin proteins, which, in turn, regulates mitochondrial velocity and positioning via variations in actin filament dynamics.

In summary, how mitochondrial movements are tightly regulated is an important question. A fluorescence excitation technique using variable penetration depths of evanescent waves was applied to investigate mitochondrial movements in living pollen tubes. The two major findings from this study are noteworthy: (a) mitochondria in pollen tubes can be classified as undergoing three types of linear movement: consistently high-speed movement, consistently low-speed movement, and variable-speed movement; (b) BDM specifically inhibited low-speed and high-speed

movements, while Jas inhibited variable-speed and high-speed movements. Our results suggest that myosin and actin filament dynamics both contribute to the speed of mitochondrial movement, while the microtubule cytoskeleton regulates mitochondrial positioning, velocities, and trajectories via its role in directing the arrangement of actin filaments.

**Acknowledgments** This work was supported by grants from the Knowledge Innovation Program of the Chinese Academy of Sciences (KJCX2-YW-L08) and A Hundred Talents Programme from the Chinese Academy of Sciences, and by the European Union Research Training Network TIPNET (project HPRN-CT-2002-00265), by Grant Agency APVT (grant no. APVT-51-002302). DCL is supported by the University of Saskatchewan and research grants from the Natural Sciences and Engineering Research Council of Canada, and the Canada Foundation for Innovation. Visits to China were supported by the Royal Society of Edinburgh International Exchange Programme.

## References

- Avisar D, Prokhnevsky AI, Makarova KS, Koonin EV, Dolja VV (2008) Myosin XI-K is required for rapid trafficking of Golgi stacks, peroxisomes, and mitochondria in leaf cells of *Nicotiana benthamiana*. *Plant Physiol* 146:1098–1108
- Basu R, Chang F (2007) Shaping the actin cytoskeleton using microtubule tips. *Curr Opin Cell Biol* 19:88–94
- Bereiter-Hahn J (1990) Behavior of mitochondria in the living cell. *Int Rev Cytol* 122:1–63
- Bove J, Vaillancourt B, Kroeger J, Hepler PK, Wiseman PW, Geitmann A (2008) Magnitude and direction of vesicle dynamics in growing pollen tubes using spatiotemporal image correlation spectroscopy and fluorescence recovery after photobleaching. *Plant Physiol* 147:1646–1658
- Chen T, Teng N, Wu X, Wang Y, Tang W, Samaj J, Baluska F, Lin J (2007) Disruption of actin filaments by latrunculin b affects cell wall construction in *Picea meyeri* pollen tube by disturbing vesicle trafficking. *Plant Cell Physiol* 48:19–30
- Cheung AY, Wu HM (2004) Overexpression of an Arabidopsis formin stimulates supernumerary actin cable formation from pollen tube cell membrane. *Plant Cell* 16:257–269
- Cheung AY, Wu HM (2008) Structural and signaling networks for the polar cell growth machinery in pollen tubes. *Annu Rev Plant Biol* 59:547–572
- de Win AHN, Pierson ES, Derksen J (1999) Rational analyses of organelle trajectories in tobacco pollen tubes reveal characteristics of the actomyosin cytoskeleton. *Biophys J* 76:1648–1658
- Demaurex N, Distelhorst C (2003) Cell biology. Apoptosis—the calcium connection. *Science* 300:65–67
- Doniwa Y, Arimura S, Tsutsumi N (2007) Mitochondria use actin filaments as rails for fast translocation in Arabidopsis and tobacco cells. *Plant Biotechnol* 24:441–447
- Dramsi S, Cossart P (1998) Intracellular pathogens and the actin cytoskeleton. *Annu Rev Cell Dev Biol* 14:137–166
- Fehrenbacher KL, Yang HC, Gay AC, Huckaba TM, Pon LA (2004) Live cell imaging of mitochondrial movement along actin cables in budding yeast. *Curr Biol* 14:1996–2004
- Hao H, Li Y, Hu Y, Lin J (2005) Inhibition of rna and protein synthesis in pollen tube development of *Pinus bungeana* by actinomycin D and cycloheximide. *New Phytol* 165:721–729
- Ligon LA, Steward O (2000) Role of microtubules and actin filaments in the movement of mitochondria in the axons and dendrites of cultured hippocampal neurons. *J Comp Neurol* 427:351–361
- Logan DC (2006) The mitochondrial compartment. *J Exp Bot* 57:1225–1243
- Logan DC, Leaver CJ (2000) Mitochondria-targeted gfp highlights the heterogeneity of mitochondrial shape, size and movement within living plant cells. *J Exp Bot* 51:865–871
- Miller KE, Sheetz MP (2006) Direct evidence for coherent low velocity axonal transport of mitochondria. *J Cell Biol* 173:373–381
- Minin AA, Kulik AV, Gyoeva FK, Li Y, Goshima G, Gelfand VI (2006) Regulation of mitochondria distribution by rhoa and formins. *J Cell Sci* 119:659–670
- Olyslaegers G, Verbelen JP (1998) Improved staining of F-actin and co-localization of mitochondria in plant cells. *J Microsc* 192:73–77
- Peremyslov VV, Prokhnevsky AI, Avisar D, Dolja VV (2008) Two class XI myosins function in organelle trafficking and root hair development in *Arabidopsis*. *Plant Physiol* 146:1109–1116
- Prokhnevsky AI, Peremyslov VV, Dolja VV (2008) Overlapping functions of the four class XI myosins in Arabidopsis growth, root hair elongation, and organelle motility. *Proc Natl Acad Sci USA* 105:19744–19749
- Reddy ASN, Day IS (2001) Analysis of the myosins encoded in the recently completed *Arabidopsis thaliana* genome sequence. *Genome Biol* 2:1–18
- Rizzuto R, Duchen MR, Pozzan T (2004) Flirting in little space: the ER/mitochondria Ca<sup>2+</sup> liaison. *Sci STKE* 2004:re1
- Semenova L, Burakov A, Berardone N, Zaliapin L, Slepchenko B, Svitkina T, Kashina A, Rodionov V (2008) Actin dynamics is essential for myosin-based transport of membrane organelles. *Curr Biol* 18:1–6
- Sheahan MB, McCurdy DW, Rose RJ (2005) Mitochondria as a connected population: ensuring continuity of the mitochondrial genome during plant cell dedifferentiation through massive mitochondrial fusion. *Plant J* 44:744–755
- Sheng X, Hu Z, Lü H, Wang X, Baluška F, Šamaj J, Lin J (2006) Roles of the ubiquitin/proteasome pathway in pollen tube growth with emphasis on MG132-induced alterations in ultrastructure, cytoskeleton, and cell wall components. *Plant Physiol* 141:1578–1590
- Sieberer BJ, Ketelaar T, Esseling JJ, Emons AM (2005) Microtubules guide root hair tip growth. *New Phytol* 167:711–719
- Sparkes IA, Teanby NA, Hawes C (2008) Truncated myosin XI tail fusions inhibit peroxisome, Golgi, and mitochondrial movement in tobacco leaf epidermal cells: a genetic tool for the next generation. *J Exp Bot* 59:2499–2512
- Staiger CJ, Sheahan MB, Khurana P, Wang X, McCurdy DW, Blanchoin L (2009) Actin filament dynamics are dominated by rapid growth and severing activity in the *Arabidopsis* cortical array. *J Cell Biol* 184:269–280
- Taraska JW, Almers W (2004) Bilayers merge even when exocytosis is transient. *Proc Natl Acad Sci USA* 101:8780–8785
- Tominaga M, Morita K, Sonobe S, Yokota E, Shimmen T (1997) Microtubules regulate the organization of actin filaments at the cortical region in root hair cells of *Hydrocharis*. *Protoplasma* 199:83–92
- Tominaga M, Kojima H, Yokota E, Orii H, Nakamori R, Katayama E, Anson M, Shimmen T, Oiwa K (2003) Higher plant myosin xi moves processively on actin with 35 nm steps at high velocity. *EMBO J* 22:1263–1272
- Trinczek B, Ebneith A, Mandelkow EM, Mandelkow E (1999) Tau regulates the attachment/detachment but not the speed of motors in microtubule-dependent transport of single vesicles and organelles. *J Cell Sci* 112:2355–2367



- Tsuboi T, Zhao C, Terakawa S, Rutter GA (2000) Simultaneous evanescent wave imaging of insulin vesicle membrane and cargo during a single exocytotic event. *Curr Biol* 10:1307–1310
- Van Gestel K, Kohler RH, Verbelen JP (2002) Plant mitochondria move on f-actin, but their positioning in the cortical cytoplasm depends on both f-actin and microtubules. *J Exp Bot* 53:659–667
- Wang Q, Kong L, Hao H, Wang X, Lin J, Samaj J, Baluska F (2005) Effects of brefeldin a on pollen germination and tube growth. Antagonistic effects on endocytosis and secretion. *Plant Physiol* 139:1692–1703
- Wang X, Teng Y, Wang Q, Li X, Sheng X, Zheng M, Samaj J, Baluska F, Lin J (2006) Imaging of dynamic secretory vesicles in living pollen tubes of *Picea meyeri* using evanescent wave microscopy. *Plant Physiol* 141:1591–1603
- Yi M, Weaver D, Hajnoczky G (2004) Control of mitochondrial motility and distribution by the calcium signal: a homeostatic circuit. *J Cell Biol* 167:661–672
- Zheng M, Beck M, Müller J, Chen T, Wang X, Wang F, Wang Q, Wang Y, Baluska F, Logan DC, Samaj J, Lin J (2009) Actin turnover is required for myosin-dependent mitochondrial movements in *Arabidopsis* root hairs. *PLoS One* 4:e5961